Am J Transl Res 2022;14(8):5466-5479
www.ajtr.org /ISSN:1943-8141/AJTR0144713

Original Article

Dexlansoprazole prevents pulmonary artery hypertension by inhibiting pulmonary artery smooth muscle cell to fibroblast transition

Qian Jiao[1*], Fangdi Zou[2*], Shiliang Li[1*], Jiawen Wang[1], Yunping Xiao[1], Zhihua Guan[1], Liang Dong[3], Jinwei Tian[4], Shengqing Li[3], Rui Wang[1], Jian Zhang[1,2], Honglin Li[1]

[1]Shanghai Key Laboratory of New Drug Design, School of Pharmacy, East China University of Science & Technology, Shanghai 200237, China; [2]School of Basic Medical Sciences, Tianjin Medical University, Tianjin 200000, China; [3]Department of Pulmonary and Critical Care Medicine, Huashan Hospital, Fudan University, Shanghai 200000, China; [4]Department of Cardiology, The Second Affiliated Hospital, Key Laboratory of Myocardial Ischemia, Harbin Medical University, Harbin 200000, Heilongjiang, China. [*]Equal contributors.

Received June 12, 2022; Accepted July 13, 2022; Epub August 15, 2022; Published August 30, 2022

Abstract: Objectives: To validate that dexlansoprazole, an anti-acid drug, can prevent pulmonary artery hypertension (PAH) in preclinical animal models and find the possible mechanism of action of dexlansoprazole for this new indication. Methods: The efficacy of dexlansoprazole to attenuate PAH in vivo was evaluated in PAH animal models. Plasma guanosine 3', 5'-cyclic phosphate (cGMP) in PAH rats was measured by enzyme linked immunosorbent assay (ELISA). To investigate the anti-PAH effect of dexlansoprazole in vitro, proliferation and migration assays of primary cultured pulmonary artery smooth muscle cells (PASMCs) were performed. Furthermore, dexlansoprazole's function on fibroblast transition of vascular smooth muscle cells (VSMC) was explored by single cell ribonucleic acid (RNA) sequencing and RNAscope. Results: Dexlansoprazole could attenuate the pathologic process in monocrotaline (MCT)-, hypoxia-induced PAH rats and SU5416/hypoxia (SuHy)-induced PAH mice. The intervention with dexlansoprazole significantly inhibited elevated right ventricular systolic pressure (RVSP), right ventricular hypertrophy, and pulmonary vascular wall thickness. Furthermore, plasma cGMP in MCT-induced PAH rats was restored after receiving dexlansoprazole. In vitro, dexlansoprazole could inhibit PASMCs' proliferation and migration stimulated by platelet derived growth factor-BB (PDGF-BB). Moreover, dexlansoprazole significantly ameliorated pulmonary vascular remodeling by inhibiting VSMC phenotypic transition to fibroblast-like cells in a VSMC-specific multispectral lineage-tracing mouse. Conclusions: Dexlansoprazole can prevent PAH through promoting cGMP generation and inhibiting pulmonary vascular remodeling through restraining PASMCs' proliferation, migration, and phenotypic transition to fibroblast-like cells. Consequently, PAH might be a new indication for dexlansoprazole.

Keywords: PAH, dexlansoprazole, pulmonary vascular remodeling, VSMC phenotype transition

Introduction

Pulmonary arterial hypertension (PAH) is a rare and malignant disease defined as mean pulmonary arterial pressure (mPAP) ≥ 25 mmHg at rest. To promote patient care earlier, the diagnosis threshold was advised to be decreased to 20 mmHg [1]. PAH is characterized by sustained pulmonary vasoconstriction and progressive vascular remodeling, which leads to right ventricular failure and premature death ultimately [1]. It is reported that elevated pulmonary vascular tone is caused by the imbalance of vasodilators such as nitric oxide (NO) [2] and prostacyclin [3, 4], and vasoconstrictors such as endothelin-1 (ET-1). Though several target therapies including endothelin receptor antagonists (ERA), prostacyclin analogs and derivatives, phosphodiesterase-5 inhibitors (PDE-5i) and soluble guanylate cyclase (sGC) stimulator are available for the treatment of PAH [5], the poor prognosis and high mortality remain unresolved [6].

Current therapies for PAH are essentially pulmonary vasodilators. However, there is a theory

that the process of pulmonary vascular remodeling drives media hypertrophy, intimal proliferation, and vascular fibrosis, which are predominant pathological feature of PAH [7]. Pulmonary artery smooth muscle cells (PASMCs) have been widely proven to participate in pulmonary vascular remodeling [8, 9]. PASMCs maintain a contractile phenotype in normal pulmonary arteries to regulate vasomotor tone and vessel caliber [10]. In response to hypoxia, PASMCs undergo an aberrant phenotypic switching to fibroblasts that induces vascular fibrosis [10]. PASMCs in vascular lesions of patients with PAH exhibit a tumor-like phenotype such as abnormal hyperproliferation, resistance to apoptosis, and altered energy metabolism [11]. Current PAH-specific therapies primarily rely upon vasodilation rather than the process of vascular remodeling.

Soluble guanylate cyclase (sGC) is an attractive target for PAH. Its activation was reported to be able to reverse pulmonary vascular remodeling [12]. To demonstrate that dexlansoprazole might stimulate sGC and inhibit PAH, we performed several *in vivo* experiments and found that dexlansoprazole increased guanosine 3', 5'-cyclic phosphate (cGMP) production and displayed good efficacy in inhibiting pulmonary hypertension and vascular remodeling in a monocrotaline (MCT)-induced rat model, a hypoxia-induced rat model and a SU5416/hypoxia (SuHy)-induced mouse model. *In vitro*, dexlansoprazole suppressed proliferation and migration of PASMCs induced by platelet derived growth factor-BB (PDGF-BB). Finally, single cell RNA-sequencing technology was applied to characterize the transcriptomes of PASMCs from Myh11 Cre^{ERT2}-ROSA floxed STOP RFP-inducible lineage tracing mice of a SuHy-induced PAH model at the single cell level. 15 clusters were identified, and two clusters with increased hyaluronidase 1 (Has1) and lumican (Lum) were characterized as fibroblast-like cells. RNA scope characterized the spatial distribution of Has1 and Lum in RFP^+ cells from lung tissues of the PAH mouse model with or without dexlansoprazole treatment. Our data showed that two clusters of fibroblast-like cells (RFP^+ Lum^+ or RFP^+ $Has1^+$) exhibited increased expression of genes involved in the SuHy-induced PAH model, which was reversed in dexlansoprazole-treated mice.

Together, our work demonstrated that dexlansoprazole, a new generation of acid suppression drug used for hydrochloric acid-related relux, could alleviate PAH progression mainly through inhibiting PASMC to fibroblast transition. Thus, dexlansoprazole may be a new option for PAH.

Materials and methods

Mice and rats

All experimental procedures conformed to the agreement of the Ethics Committee on Laboratory Animal Care and the Guidelines for the Care and Use of Laboratory Animals in Shanghai, China and approved by Laboratory Animal Ethics Committee of East China University of Science and Technology (ECUST-2022-074). C57BL/6 mice and Sprague-Dawley (SD) rats were obtained from Shanghai Sipprbk Laboratory Animal Co., LTD (Shanghai, China). Myh11-CreERT2 mice (#019079) and Gt (ROSA) 26Sortm9 (CAG-tdTomato) Hze (R26mTmG/+) mice (#007909) were purchased from Jackson Laboratory. Mice used for SuHy-induced PAH model establishment were C57BL/6 background. All animals were housed in an environment with a 12 h-light/dark cycle, and provided with enough water and food.

Materials

Dimethylsulfoxide (DMSO) and paraformaldehyde (PFA) were from Sigma Aldrich (St Louis, MO, USA). MCT was purchased from Biopurify Phytochemicals Ltd. (Chengdu, China) and dissolved as 12 mg/mL in normal saline with 20% (*v/v*) absolute ethanol. Antibodies against Lum and α-smooth muscle actin (α-SMA) were obtained from Abcam (Cambridge, UK) and Has1 antibody was from Thermo Scientific (Waltham, US). SU5416 was purchased from MCE (NJ, US). Dulbecco's modified Eagle's medium (DMEM) was purchased from Hyclone Laboratories (Logan, UT, USA). Fetal bovine serum (FBS), GlutaMAX, and trypsin-EDTA were from Gibco BRL (Grand Island, NY, USA). 3-(4, 5-Dimethythiazol-2-yl)-2, 5-diphenyl-tetrazolium bromide (MTT) was purchased from Sangon Biotech (Shanghai, China). Transwell system was obtained from Corning (Cypress, CA). Recombinant rat PDGF-BB was from Absin Bioscience Inc. (Shanghai, China).

Culture of primary rat PASMCs

Primary rat PASMCs were isolated from the first branch of the pulmonary artery of SD rats. Briefly, 6-week-old SD rats were anaesthetized with urethane (20%, *w/v*%, ip). Then, the first branch of the pulmonary artery was removed and washed with D-Hanks for several times. The adventitia was separated carefully and the intima was shaved lightly. The tissue was cut into small pieces and cultured in medium containing DMEM, 20% FBS, 100 $U \cdot mL^{-1}$ penicillin, and 100 $mg \cdot mL^{-1}$ streptomycin in a humidified atmosphere of 95% air and 5% CO_2 at 37°C. Fresh medium was replaced every 3 days.

Cell proliferation assay

MTT assay was performed to detect proliferation of PASMCs. Cells were seeded in a 96-well cell culture plate at a density of 3000 cells per well. Proliferation of the PASMCs was induced by PDGF-BB (20 ng/mL) in DMEM with or without 5-100 μmol/L dexlansoprazole pre-treatment (2 h). After 48 h, 10 μL MTT solution (5 mg/mL) was added into each well and co-incubated for 4 h at 37°C to form formazan crystals, which were subsequently dissolved by replacing culture medium with 120 μL DMSO. Finally, OD 490 nm absorbance was measured using a Synergy 2 multi-mode microplate reader (BioTek, USA).

Cell migration assay

For wound healing assay, PASMCs (2×10^5 cells/mL) were seeded into a 12-well plate. On the second day, a 10-μL pipette tip was drawn across the center of the well to make a straight scratch. After being rinsed with PBS for three times, DMEM containing 2% FBS plus dexlansoprazole and PDGF-BB (20 ng/mL) were added to each well. Cell migration was detected with a light microscope (Nikon, Tokyo, Japan) after incubation for 0, 12, or 24 h. The migration width was analyzed for comparison.

For transwell assay, PASMCs (1×10^5 cells) were loaded onto the upper chamber while DMEM containing dexlansoprazole (100 μM) and/or PDGF-BB (20 ng/mL) were added into the lower chamber. After co-culturing at 37°C for 6 h, the cells that had migrated into the lower chamber were fixed with 4% PFA and stained by 0.1% crystal violet while the non-migrated cells were removed. Five random fields were randomly chosen for observation and photography.

cGMP assay

To measure the cGMP concentration in plasma, blood sampling from the abdominal aorta was taken after the last administration. Plasma was obtained by centrifuging the clotted blood at 3500 rpm for 10 min (Eppendorf, Germany). Enzyme linked immunosorbent assay (ELISA) for rat plasma cGMP was carried out using a commercial kit (Elabscience, China), in accordance with the manufacturer's protocol.

MCT-induced PAH rats model

Male SD rats (180-200 g) were randomly divided into six groups: (1) Control group, (2) MCT group, (3) MCT + selexipag (po, 1 mg/kg twice daily), (4) MCT + low dose dexlansoprazole (po, 5 mg/kg once daily), (5) MCT + medium dose dexlansoprazole (po, 10 mg/kg once daily), and (6) MCT + high dose dexlansoprazole (po, 20 mg/kg once daily), 6 rats/group. On the first day, rats of five of the groups received a single injection of MCT (60 mg/kg) subcutaneously, while one group was given saline and served as controls. Subsequently, rats in different groups were given selexipag, dexlansoprazole, or vehicle respectively for 21 days.

Hypoxia-induced PAH rat model

After 1 week of adaptation, 48 male SD rats were divided into 6 groups (n = 8): (1) normoxia group, (2) hypoxia group, (3) hypoxia group + low dose dexlansoprazole (po, 5 mg/kg once daily), (4) hypoxia group + medium dose dexlansoprazole (po, 10 mg/kg once daily), (5) hypoxia group + high dose dexlansoprazole (po, 20 mg/kg once daily) and (6) hypoxia group +sidenafil (po, 10 mg/kg once daily). Rats in the normoxic group and other groups were respectively housed in ambient barometric pressure and a hypobaric hypoxia chamber (10% O_2) 8 h/day for 28 days.

Hemodynamic measurements for rats

The right external jugular vein of rats was separated after being injected with 20% (*w/v*) urethane at the end of last drug administration. Then a 0.5% heparin-filled blunt-ended PE 50

catheter connected to PowerLab Data Acquisition System (AD Instruments, Australia) was positioned into the right ventricle through the superior vena cava and right atrium. Next, the right ventricular systolic pressure (RVSP) was recorded.

SU5416/hypoxia-induced PAH mouse model

Male mice (8-week-old) were injected with SU5416 (20 mg/kg) subcutaneously, and were then exposed to hypoxia (10% O_2) for 4 weeks. SU5416 was suspended in carboxymethylcellulose (CMC) solution (0.5% [*w/v*] CMC sodium, 0.9% [*w/v*] sodium chloride, 0.4% [*v/v*] polysorbate 80, and 0.9% [*v/v*] benzyl alcohol in deionized water). After being hypoxia-induced for 2 weeks, dexlansoprazole was administrated at a dose of 10 mg/kg/day and cells remained in a normoxic environment. 2 weeks later, mice were anesthetized by intraperitoneal injection with tribromoethanol (dissolved in amylene alcohol at storage concentration of 1 g/mL, diluted with dd water at a working concentration of 12 mg/mL, and dosage was 192 mg/kg), then laid in a supine position on a heating platform and ventilated through a transtracheal catheter. A left parasternal incision was made and small parts of the ribs were carefully resected. A 1.2-F (for mice) micro-tip pressure transducer catheter (Millar Instruments, Houston, TX, USA) was carefully inserted into the right ventricular apex, and Right ventricular systolic pressure (RVSP) was continuously recorded for 2 min using the PowerLab Data Acquisition System.

Histological analysis

The heart after removal of residual blood, was divided into right ventricle (RV) and left ventricle (LV) plus septum (S). Then RV and LV plus S were weighed respectively, to calculate the weight ratio of RV/(LV+S). The right lung tissues were embedded in paraffin and cut into 5-μm slices followed by haematoxylin-eosin (H&E) staining. 14 or 15 pulmonary arterioles in each sample (categorized as < 50 μm and > 50 μm in diameter) were measured by Image-Pro Plus software 6.0.

Immunostaining

For immunofluorescence, lung tissue sections were blocked in TBST containing 12% Bovine serum albumin (BSA), dissolved in phosphate buffered solution (PBS) containing 0.01% TritonX-100, and stained with primary antibodies (1:2000) overnight at 4°C. After incubation with Alexa Fluor-conjugated secondary antibodies (Invitrogen, Carlsbad, CA) staining, nuclear staining was performed with DAPI (5 mg/mL, Invitrogen, Carlsbad, CA). Then sections were mounted with ProLong® Gold Antifade Reagent (Invitrogen, Carlsbad, CA) on glass slides and were visualized using a confocal microscope (Nikon, A1R, Japan).

For immunohistochemistry, lung tissue sections were stained with α-SMA mouse antibody, followed by horseradish peroxidase (HRP)-conjugated anti-mouse IgG (Servicebio, China). Slides were developed with DAB peroxidase substrate (Servicebio, China) and counterstained with hematoxylin. Stained sections were observed under an optical microscope (Leica, China) and photographed.

Tamoxifen-induced genetic lineage tracing

Tamoxifen was dissolved in corn oil to 20 mg/mL. and gave to Myh11-CreERT2 mice at day 1, day 3, and day 5 at a dose of 200 mg/kg (po). Then samples were collected at indicated time points.

Single cell sequencing

BD Resolve system (BD Genomics, Menlo Park, CA) was applied to capture transcriptomic information of single pulmonary vascular smooth muscle cells (VSMCs) from PAH mice. Lung tissues from PAH mice were digested and dissociated into single cells enzymatically, and then flow cytometry was used to sort RFP^+ $Lgr6^-$ VSMCs [13]. Single cell sequencing was processed as previously described [14].

Single cell capture was acquired by random distribution of a single cell suspension across > 200,000 microwells with a limited dilution approach. Beads combined with oligonucleotide barcodes were added to saturation so that a bead was paired with a cell in a microwell. Poly-adenylated RNA molecules were hybridized to the beads in cell lysis buffer. Beads were collected for complementary deoxyribonucleic acid (cDNA) synthesis and the 5' end of each cDNA had added to it, a molecular index and cell label to indicate cell source. The tran-

scriptome libraries were prepared using the BD Resolve single cell whole transcriptome amplification workflow. Next, second strand cDNA was synthesized and followed by ligation of adaptor for universal transcriptome amplification. Sequencing libraries were prepared with random priming PCR of the whole transcriptome amplification products. Sequencing libraries were quantified with a High Sensitivity DNA Chip (Agilent, USA) on a Bioanalyzer 2100 and the Qubit High Sensitivity DNA Assay (Thermo Fisher Scientific, USA). 1.5 pM of each sample in the library was added to a NextSeq 500 system and sequenced using High Output sequencing kits (75 × 2 bp) (Illumina). The BD Resolve analysis pipeline was used for processing sequencing data. Molecular indices and cell labels were identified and genes were determined by alignment against the gene code comprehensive reference. Single cell sequencing and data analysis were processed by Genechem Co. (Shanghai, China).

RNAscope assay procedure for RNA detection

RNAscope Assay kit was purchased from ACD Bio-Techne (Newark, US). For lung tissues, tissue sections in 5-μm thickness were deparaffinized in xylene, followed by dehydration in an ethanol series. Tissue sections were then placed into citrate buffer (10 nmol/L, pH = 6) at boiling temperature (100°C to 103°C) in a hot plate for 15 min. After rinsing by deionized water, 10 μg/mL protease (Sigma-Aldrich, St. Louis, MO) was added and co-incubated at 40°C for 30 min in a HybEZ hybridization oven (Advanced Cell Diagnostics, Hayward, CA). Hybridization with target probes, preamplifier, amplifier, and labeled probe and chromogenic detection were as described above for cultured cells. To prepare and fix FFPE samples optimally, assay conditions like the pretreatment conditions were explored according to American Society of Clinical Oncology/College of American Pathologists (ASCO/CAP) guidelines [14] (10% neutral buffered formalin for 6 to 72 h at room temperature).

Positive and negative controls were performed in parallel to get interpretable results. The endogenous housekeeping gene UBC and bacterial gene dapB were used as positive control and negative control. Photos were taken with a Confocal Laser Scanning Microscope (Carl Zeiss, Oberkochen, Germany).

Statistical analysis

All data were expressed as the mean ± SEM. Data were analyzed using SPSS software, version 25.0. The Student's *t* test was performed to compare 2 data sets, while one-way analysis of variance (ANOVA) was to assess three or more groups. $P < 0.05$ was regarded as significant.

Results

Dexlansoprazole induced cGMP production and suppressed the progression of MCT-induced PAH in rats

sGC, a unique endogenous receptor of NO, is a clinically validated target for PAH. On binding with NO, sGC catalyzes the conversion from guanosine triphosphate (GTP) to cGMP, which can induce vasodilation, suppress VSMC proliferation and vascular fibrosis [15]. Previously we found that dexlansoprazole might bind to sGC [16]. Further research indicated that a decreased level of plasma cGMP in MCT-treated group was moderately reversed by dexlansoprazole treatment for 3 weeks ($P < 0.05$ *vs.* MCT) (**Figure 1A**). We also examined the therapeutic effects of dexlansoprazole on pulmonary hemodynamic and pulmonary vascular remodeling in MCT-treated rats (**Figure 1B**). Dexlansoprazole (5 mg/kg, 10 mg/kg and 20 mg/kg) significantly attenuated the increase in RVSP [(67.51 ± 9.11) mmHg, (67.20 ± 4.18) mmHg and (55.95 ± 4.37) mmHg *vs.* MCT (59.29 ± 8.17 mmHg), $P < 0.05$, $P < 0.05$ and $P < 0.01$] (**Figure 1C**). After MCT challenged for 3 weeks, the MCT-treated group showed an increased ratio of RV/(LV + S) ($P < 0.001$ *vs.* CON), which was reversed by dexlansoprazole at a dosage of 20 mg/kg ($P < 0.05$ *vs.* MCT) (**Figure 1F**). Selexipag, a newly approved selective prostacyclin receptor agonist [16], was set as a positive control in this experiment. Additionally, dexlansoprazole decreased pulmonary vascular wall thickness and α-SMA expression, indicating that dexlansoprazole could alleviate MCT-induced pulmonary vascular remodeling (**Figure 1D**, **1E**).

Dexlansoprazole ameliorated hypoxia-induced PAH in rats and SuHy-induced PAH in mice

We next explored the pulmonary hemodynamic and histologic changes of rats exposed to a hypoxic environment and dexlansoprazole (**Fi-**

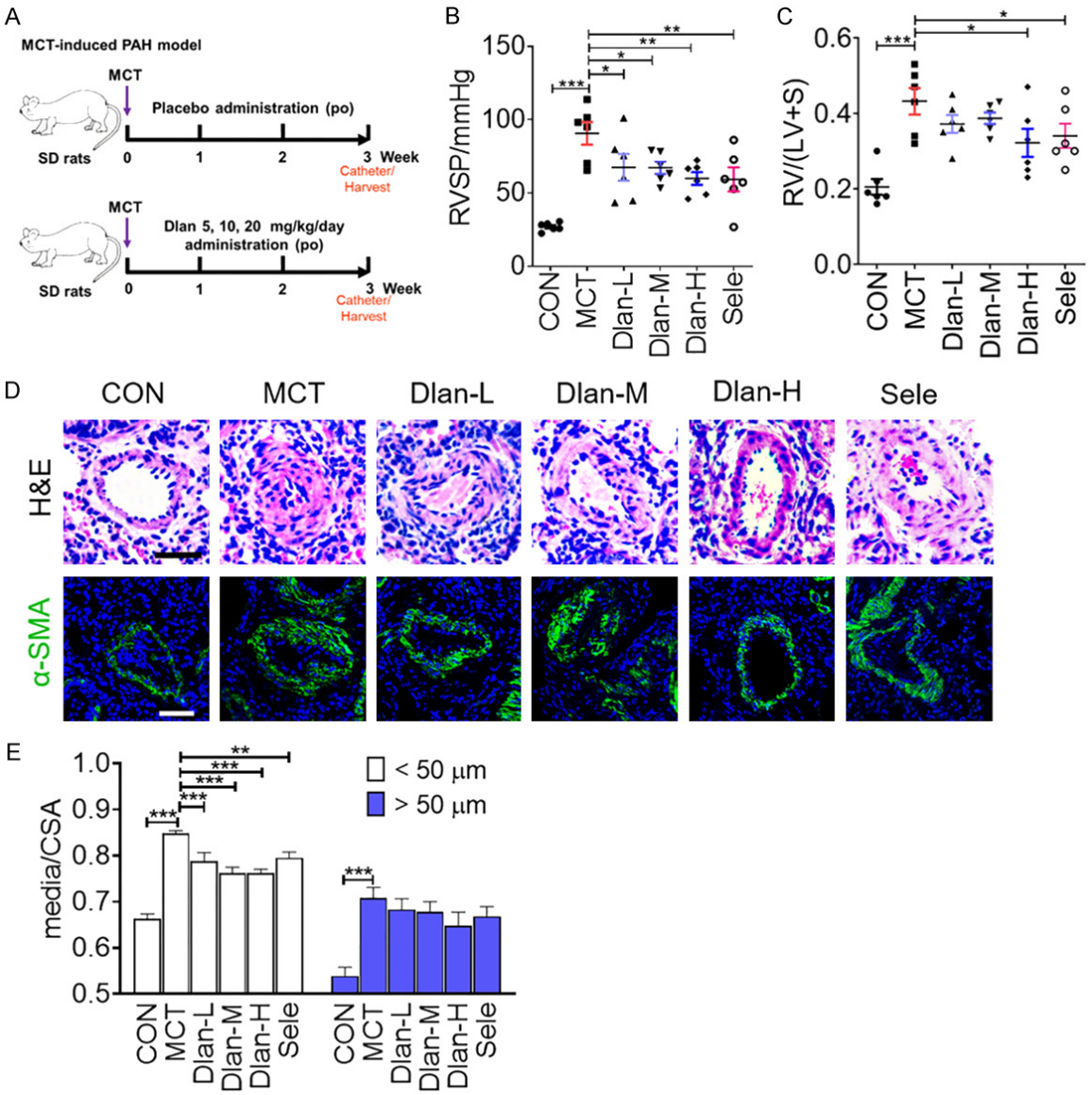

Figure 1. Dexlansoprazole prevents the development of MCT-induced PAH in rats. A. Plasma cGMP concentration from MCT induced PAH rats. *P < 0.05; ***P < 0.001 (n = 6). B. Protocol for administration of dexlansoprazole to MCT-challenged rats. C. Effect of dexlansoprazole administration on RVSP in rats induced by MCT with dexlansoprazole treatment. *P < 0.05; **P < 0.01; ***P < 0.001 (n = 6). D. Representative H&E-stained lung sections and immunofluorescence images of α-smooth muscle actin (α-SMA; green) from rats injected with MCT with dexlansoprazole treatment. Scale bars: 50 μm for 20x. E. Quantification of the ratio of vascular media thickness to total vessel size for rats exposed to MCT with dexlansoprazole treatment. *P < 0.05; **P < 0.01; ***P < 0.001 (n = 6). CON: control; MCT: monocrotaline; Dlan-L: dexlansoprazole (5 mg/kg, po) treatment; Dlan-M: dexlansoprazole (10 mg/kg, po) treatment; Dlan-H: dexlansoprazole (20 mg/kg, po) treatment; Sele: selexipag (1 mg/kg, bid); Rio: riociguat (10 mg/kg, po). F. RV/(LV + S) in rats induced by MCT with dexlansoprazole treatment. *P < 0.05; ***P < 0.001 (n = 6). Data represent mean ± SEM. Statistical significance was evaluated by one-way ANOVA. CSA indicates cross-sectional area.

gure 2A). Daily administration of high dosage dexlansoprazole (20 mg/kg, po) for 28 days notably ameliorated hypoxia-induced PAH by reducing RVSP to 57.57 ± 3.96 mmHg (P < 0.05 *vs.* hypoxia) (**Figure 2B**). Furthermore, dexlansoprazole modestly suppressed hypoxia-induced pulmonary vascular thickening (**Figure 2D**), as indicated by decreased α-SMA expression (**Figure 2D**) and pulmonary artery wall thickness (media/CSA) (**Figure 2E**).

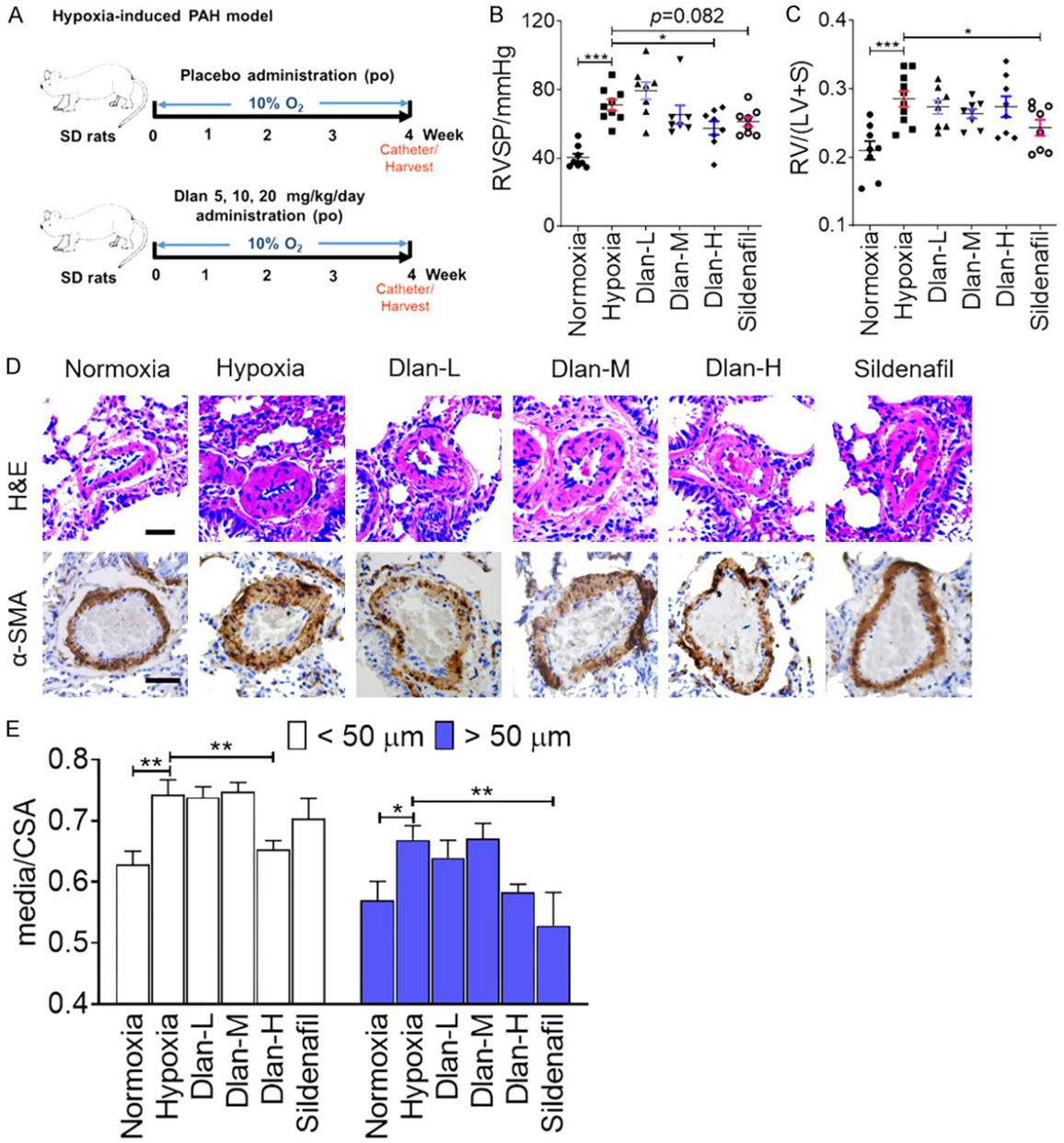

Figure 2. Dexlansoprazole suppresses the progression of hypoxia-induced PAH in rats. A. Protocol for hypoxia-induced PAH in rats. B. RVSP in rats exposed to hypoxia with dexlansoprazole treatment. *P < 0.05; ***P < 0.001 (n = 8). C. RV/(LV + S) in rats exposed to hypoxia with dexlansoprazole treatment. *P < 0.05; ***P < 0.001 (n = 8). D. Representative H&E-stained lung sections and immunostained images of α-SMA (brown) from rats exposed to hypoxia with dexlansoprazole treatment. Scale bars: 50 μm for 20x. E. Quantification of the ratio of vascular media thickness to total vessel size for rats exposed to hypoxia with dexlansoprazole treatment. *P < 0.05; **P < 0.01; ***P < 0.001 (n = 6). Normoxia: 21% O_2; Hypoxia: 10% O_2; Dlan-L: dexlansoprazole (5 mg/kg, po) treatment; Dlan-M: dexlansoprazole (10 mg/kg, po); Dlan-H: dexlansoprazole (20 mg/kg, po). Sildenafil: 10 mg/kg, po. Data represent mean ± SEM. Statistical significance was evaluated by one-way ANOVA.

A SuHy-induced PAH mice model was established to further assess the therapeutic potential of dexlansoprazole for PAH (**Figure 3A**). Mice in the model group developed a significant elevation in RVSP (**Figure 3B**) and RV/LV + S (**Figure 3C**) compared to placebo mice exposed to normoxia. Likewise, dexlansoprazole (10 mg/kg and 20 mg/kg) exhibited a significant reduction in RVSP [10 mg/kg (22.50 ± 1.94) mmHg, 20 mg/kg (20.91 ± 2.70) mmHg

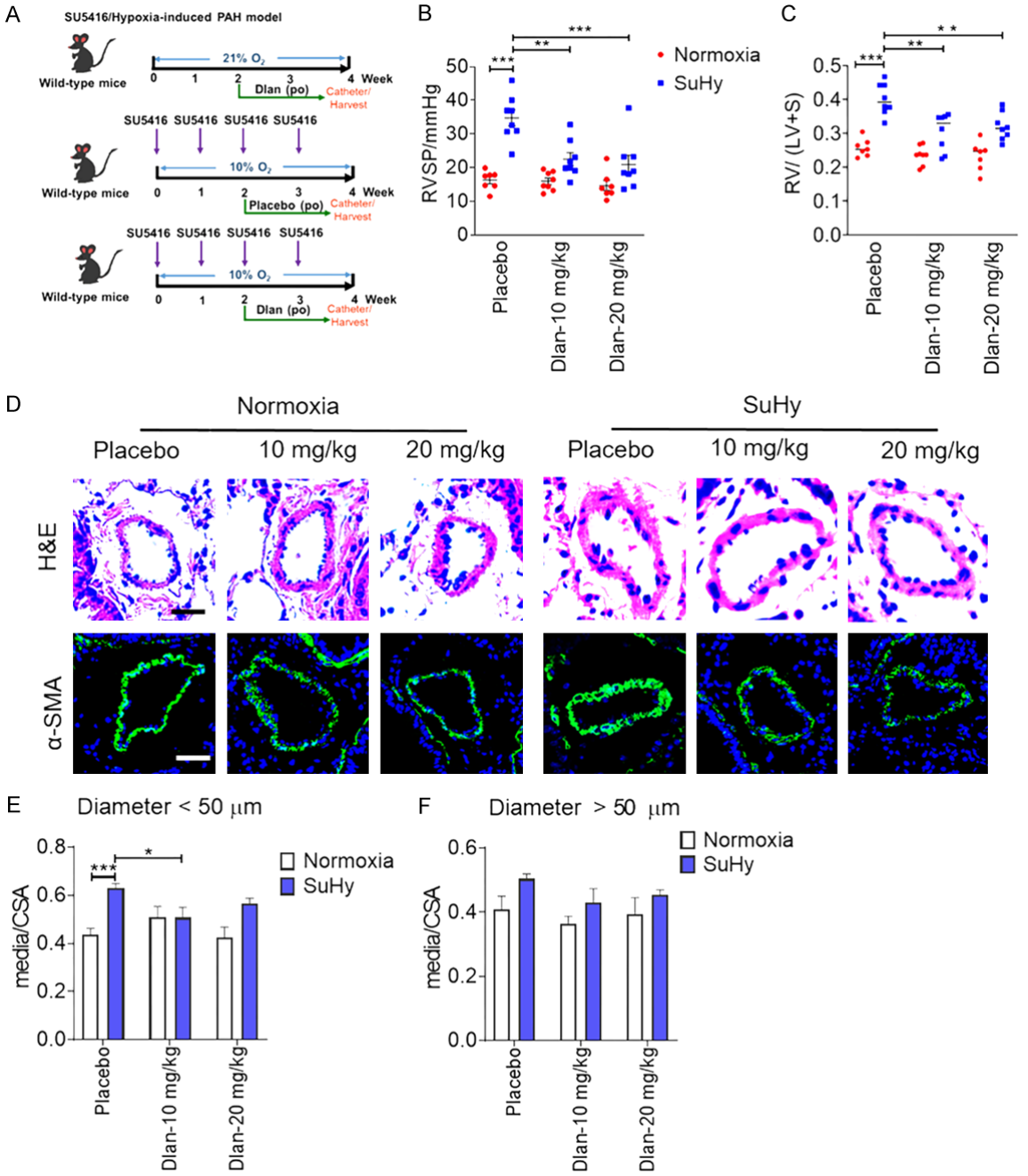

Figure 3. Dexlansoprazole attenuates SU5416/hypoxia-induced PAH in mice. A. Protocol for HySu-induced PAH in mice. B. RVSP in mice exposed to SU5416/hypoxia with dexlansoprazole treatment. **P < 0.01; ***P < 0.001 (n = 7-8). C. RV/(LV + S) in mice exposed to SU5416/hypoxia with dexlansoprazole treatment. **P < 0.01; *** P < 0.001 (n = 8). D. Representative H&E sections and immunofluorescence images of α-SMA (green) from rats exposed to SU5416/hypoxia with dexlansoprazole treatment. Scale bars: 50 μm for 20x. E. Quantification of the ratio of vascular media thickness to total vessel size for mice exposed to SU5416/hypoxia with dexlansoprazole treatment (diameter < 50 μm); *P < 0.05, ***P < 0.001 (n = 6). F. Quantification of the ratio of vascular media thickness to total vessel size for mice exposed to SU5416/hypoxia with dexlansoprazole treatment (diameter > 50 μm) (n = 6). Scale bars: 50 μm. Normoxia: 21% O_2; Hypoxia: 10% O_2; SU5416: 20 mg/kg, ip. Data represent mean ± SEM. Statistical significance was evaluated by one-way ANOVA.

vs. SuHy (34.76 ± 2.37) mmHg, P < 0.01 and P < 0.001] (**Figure 3B**). Consistently, dexlansoprazole treatment reduced RV/(LV + S) [10 mg/kg (0.30 ± 0.02), 20 mg/kg (0.32 ± 0.01) *vs.*

SuHy (0.40 ± 0.02) mmHg, P < 0.01] (**Figure 3C**) and α-SMA expression (**Figure 3D**). Intriguingly, dexlansoprazole was shown to inhibit wall thickness of vessels with diameter < 50 μm, indicating its effect on attenuating vascular remodeling in small pulmonary arteries. (**Figure 3E**, **3F**).

Dexlansoprazole inhibited PDGF-BB-induced excessive proliferation and migration of PASMCs

The uncontrolled proliferation and migration of PASMCs are crucial events in vascular remodeling. Thus, we performed MTT assay to evaluate cell viability in the absence or presence of dexlansoprazole (5, 10, 50, 100 μmol/L). The data showed that dexlansoprazole decreased PDGF-BB-induced rat PASMCs proliferation in a concentration-dependent manner but had little influence when incubated with PASMCs alone (**Figure 4A**, **4B**). Next, we monitored the migration of rat PASMCs treated with dexlansoprazole by a traditional scratch wound healing assay. Dexlansoprazole concentration-dependently reduced PDGF-BB-stimulated migration width after 12 h and 24 h incubation (**Figure 4C**, **4D**). To rule out the impact of cell proliferation, a transwell assay was performed and consistently showed that dexlansoprazole (100 μmol/L) strikingly attenuated the migration ability of PASMC treated with PDGF-BB (about 50% suppression compared with untreated PDGF-BB) (**Figure 4E**, **4F**).

Dexlansoprazole inhibited VSMC to fibroblast transition in SuHy-induced PAH in mice

A genetic lineage tracing system for Myh11-expressing cells by crossing Myh11-CreERT2 with R26-tdTomato mouse was applied for labeling of smooth muscle lineage (**Figure 5A**). To examine the efficiency of VSMC-specific RFP expression in lineage tracing mice, Myh11-CreER R26-tdTomato mice received tamoxifen (Tam) and tissues were collected after 6 days for induction efficiency analysis and after 28 days for single cell sequencing (**Figure 5B**). Immunostaining showed co-localization of Myh11 and RFP in both pulmonary arteries and airways (**Figure 5C**). It has been reported that Lgr6 was specially expressed in airway smooth muscle cells [17]. Thus, RFP^+ $Lgr6^-$ cells were defined as pulmonary VSMCs and sorted by flow cytometry. Flow cytometric analysis showed that 21.7% of cells were labeled with RFP in total lung lysate, whereas 50.7% of RFP^+ cells were in the absence of Lgr6 expression, which were identified by scRNA-seq (**Figure 5D**). 4933 cells were obtained, and on average, 1565 genes were detected per cell. Based on Uniform Manifold Approximation and Projection (UMAP) analysis, we identified 15 clusters including endothelial-like (clusters 0, 1, 4, 5) and fibroblast-like populations (clusters 2, 3, 10) based on marker gene expression (**Figure 5E**). Endothelial cell markers Pecam1 (Platelet endothelial cell adhesion molecule 1) and Cdh5 (Cadherin 5) and (**Figure 5F**, **5G**). and fibroblast markers Dcn (Decorin) and Col1a1 (Collagen 1a1) were highly expressed but there was a decrease in Myh11 expression (**Figure 5H**, **5I**). Further GO pathway analysis revealed that ECM-receptor interaction and focal adhesion related pathways were enriched in fibroblast-like cells (Cluster 2, 3, 10), indicating the function of these cells in vascular fibrosis (Figure S1). Mapping the fate of RFP^+ $Lgr6^-$ cells revealed VSMCs as the predominant source of endothelial-like and fibroblast-like cells that populate remodeled pulmonary vessels in the chronic hypoxia mouse model. Moreover, to reveal the positional information of $Myh11^+$ cell-originated fibroblast-like cells in the vessel walls, we detected the Lum and Has1 profile in RFP^+ cells. These were reported to be crucial for fibroblast characteristics [18]. Lung tissue sections were applied for RNAscope technology of Lum or Has1. We found that a subset of RFP^+ cells in the vessel wall was colocalized with Lum and Has1 in SuHy-induced PAH mice, of which the expression was impaired after treatment with dexlansoprazole (**Figure 5J**, **5K**). Thus, dexlansoprazole inhibited VSMC transition to fibroblast-like cells and vascular fibrosis in SuHy-induced PAH in mice.

Discussion

Pulmonary artery hypertension (PAH) is a rare but life-threatening cardiopulmonary disease. The mortality rate caused by PAH is about 15% in the first year and the median survival is only 2-3 years [19], though anti-PAH drugs have given substantial progress in recent years. The efficacy of current drugs for PAH is limited on account of the complex pathology [20]. It is urgent to develop effective medicines to prolong the life span and improve PAH patients' life

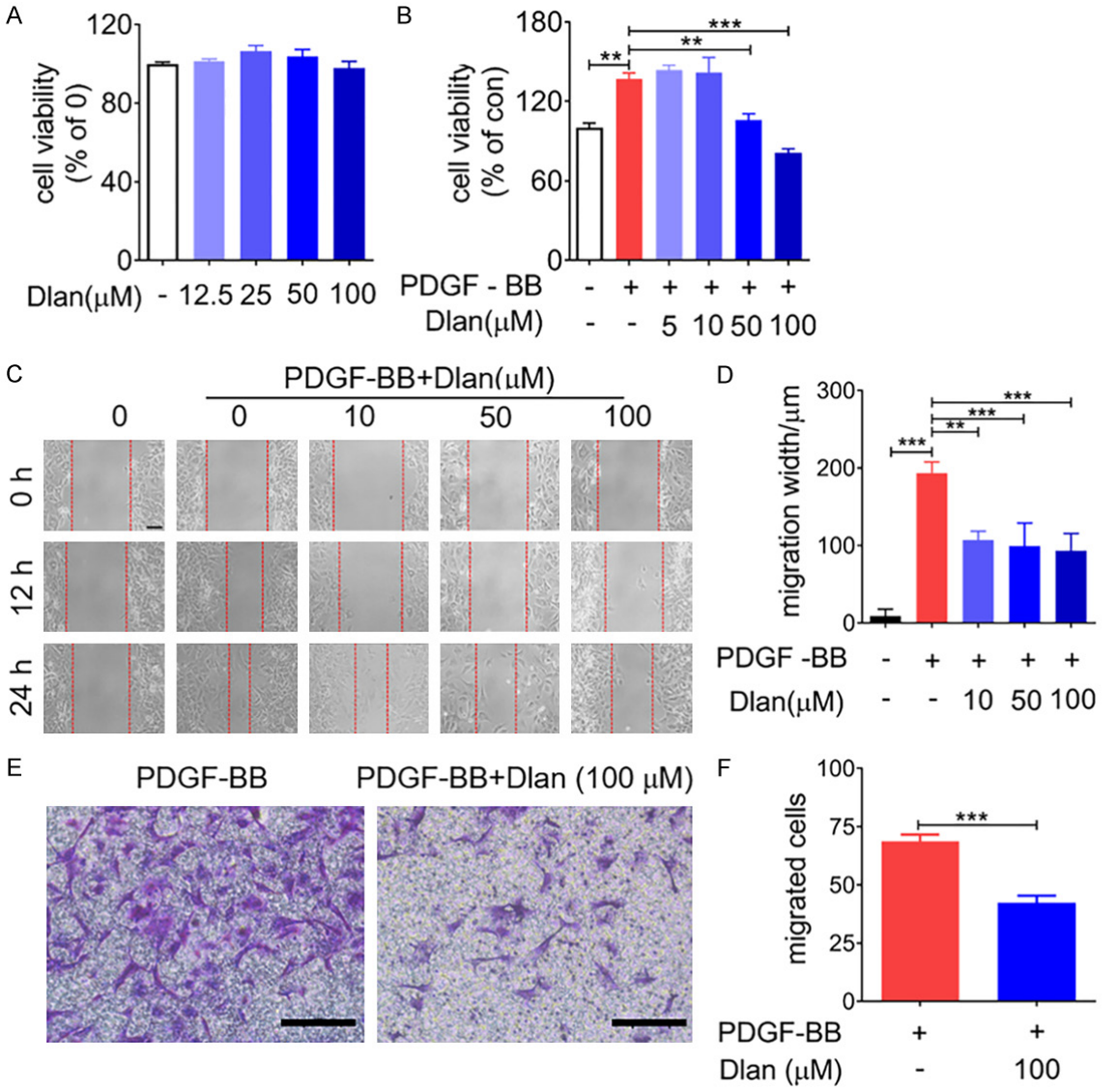

Figure 4. Dexlansoprazole inhibits PDGF-BB induced overproliferation and migration of PASMCs. A. Rat PASMCs were cultured with dexlansoprazole for 24 h and cell viability was measured by MTT assay. Proliferation rate without dexlansoprazole served as 100% (n = 3). B. Rat PASMCs were cultured with and PDGF-BB (20 ng/mL) and dexlansoprazole for 24 h. Cell viability was measured by MTT assay. The proliferation rate without PDGF-BB or dexlansoprazole served as 100%. **P < 0.01; ***P < 0.001 (n = 3). C. Representative photomicrographs of wound healing assay. D. Quantification of migration width in wound healing assay. **P < 0.01; ***P < 0.001 (n = 3). E. Representative photomicrographs of transwell migration chamber assay. F. Quantification of migrated cells in transwell assay. Scale bars: 50 μm for 10x and 200 μm for 10x. ***P < 0.001 (n = 5).

quality. sGC is a new therapeutic target for PAH sinceits stimulation can induce vasodilation. We have previously found that sGC might be a target of dexlansoprazole [16]. cGMP generated from GTP catalyzed by sGC is a critical second messenger in the NO pathway. Therefore, we evaluated cGMP generation in plasma from MCT-induced PAH rats. Interestingly, dexlansoprazole could significantly increase cGMP concentration ($P < 0.05$) while preventing experimental PAH.

PAH rodent animal models have been widely used for further understanding of this disease and pharmaceutical development. Our data displayed that dexlansoprazole significantly reduced abnormally increased RVSP and RV hypertrophy in rodent PAH models (MCT-in-

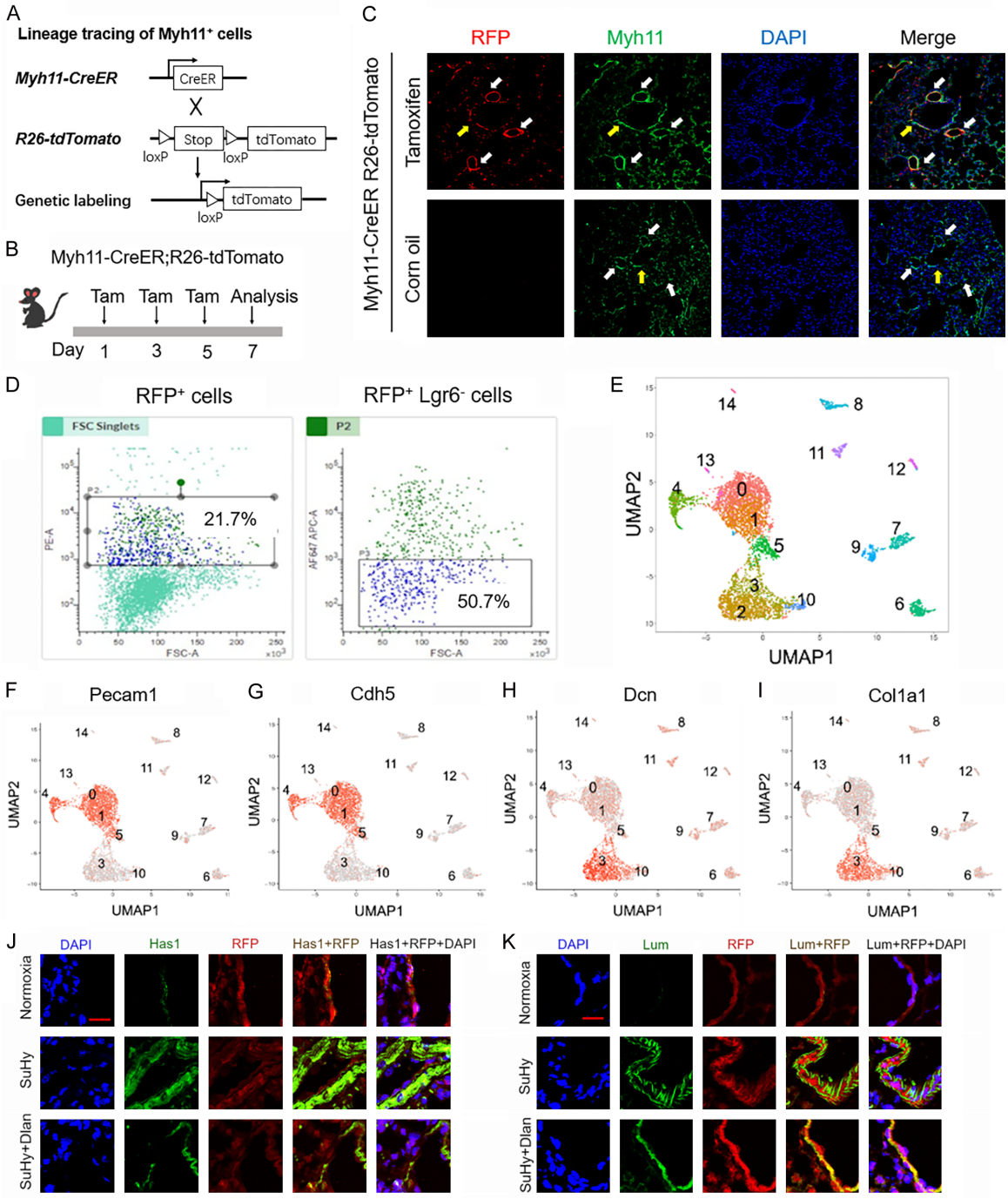

Figure 5. scRNA-seq analysis of pulmonary artery smooth muscle cells. A. Schematic showing genetic lineage tracing by Myh11-CreER. B. Sketch of the experimental design. C. Immunostaining for tdTomato and Myh11 on lung tissues (20x). D. Flow cytometry quantification of the number of tdTomato$^+$ cells and tdTomato$^+$ Lgr6$^-$ cells. E. Visualization of unsupervised clustering in a Uniform Manifold Approximation and Projection (UMAP) plot of 4933 RFP$^+$ Lgr6$^-$ cells isolated from lung tissue. F, G. Gene expression pattern of common endothelial marker genes in cluster 0, 1, 4, 5. H, I. Gene expression pattern of fibroblast marker in cluster 2, 3, 10. J, K. Detection of the mRNA of Has1 and Lum in the pulmonary artery using RNAscope in situ hybridization. Scale bars: 10 μm for 20x

duced, hypoxia-induced PAH in rats and SuHy-induced PAH in mice). Lung morphology and α-SMA staining revealed that pulmonary vascular remodeling was alleviated after dexlansoprazole intervention. Dexlansoprazole is a classical proton pump inhibitor (PPI), which was approved for use in 2009 for the treatment of gastroesophageal reflux disease (GERD) throu-

gh the blockage of H^+/K^+-ATPase in the parietal cells [21]. PPIs are reported to have few serious side effects and can be even used during pregnancy. Recent studies have shown that PPIs possess various biological functions that might be irrelevant to acid suppression [22-24]. Some retrospective studies found PPIs could improve outcomes in idiopathic pulmonary fibrosis (IPF) [25]. The conditional use of PPIs for treating IPF has been recommended in evidence-based guidelines. Esomeprazole was also reported to possess anti-fibrotic activity, reduce collagen expression in the lung tissue and inhibit progression of bleomycin-induced lung inflammation and fibrosis in rats [26].

VSMCs, fibroblasts and endothelial cells have been shown to participate in vascular fibrosis, which is one of the key pathogenic events of PAH [27, 28]. Multiple smooth muscle cell subpopulations existing in the pulmonary artery are charactered by plasticity [29]. We found that RFP^+ cell-originated fibroblast-like cells mainly consist of fibroblasts, smooth muscle cells and myofibroblasts. It was reported that $Has1^+$ fibroblasts were found restricted to the immediate subpleural region, whereas $PLIN2^+$ and Lum^+ fibroblasts appeared diffusely to parenchymal regions in pulmonary fibrosis [18]. Single-cell RNA sequencing and genetic lineage tracing were applied to display the relation of RFP^+ $Lgr6^-$ cell-derived $Has1^+$ and Lum^+ fibroblasts in vascular fibrosis after dexlansoprazole inhibition. Moreover, we found that the expansion of a specialized subpopulation of SMCs was accompanied by the transient loss of Myh11 expression during the vascular remodeling process, which is consistent with a study reported previously [30].

Hypoxia exposure also increased endothelial to mesenchymal transition (EndoMT) [31], which is a process whereby an endothelial cell (EC) undergoes phenotypic transition towards a mesenchymal cell [32, 33]. Limited overlap between lineage-traced ECs and SMCs markers was shown in a monocrotaline pyrrole/pneumectomy model by lineage tracing study [34]. This is consistent with our previous finding that $Myh11^+$ $Lgr6^-$ cell-derived endothelial-like cells are a heterogamous population that includesECs and mesenchymal cells [35].

Several treatment options identified for PAH have played a critical role to promote patients' life quality [36]. However, PAH is still a threat, with high mortality. Riociguat, an sGC stimulator, is a novel targeted therapy for PAH. Hypotension is an adverse effect of riociguat [37], since its non-selectively targets the pulmonary arteries. Women are required to participate in the Risk Evaluation and Mitigation Strategy (REMS) program due to the teratogenicity of riociguat [38]. In contrast to riociguat, PPIs are well tolerated and safe even in pregnancy [39, 40]. In this study, dexlansoprazole could increase cGMP production in plasma, indicating that this compound might be able to activate sGC. In the present study, we discovered that dexlansoprazole inhibited $Myh11^+$ VSMC transition to fibroblast which has not often been reported. In light of our current findings, further research is needed to elucidate the exact molecular anti-fibrosis mechanism.

Acknowledgements

This work was supported by the National Natural Science Foundation of China (grants, 81825020 to HLL, 81803437 and 82173690 to SLL, 81771513 to JZ); the Fundamental Research Funds for the Central Universities; Jian Zhang is sponsored by Young Elite Scientists Sponsorship Program by Tianjin (TJSQNTJ-2018-10). Honglin Li is also sponsored by the National Program for Special Supports of Eminent Professionals and National Program for Support of Top-Notch Young Professionals.

Disclosure of conflict of interest

None.

Address correspondence to: Drs. Rui Wang, Jian Zhang and Honglin Li, Shanghai Key Laboratory of New Drug Design, School of Pharmacy, East China University of Science and Technology, Shanghai 200237, China. Tel: +86-21-64250823; Fax: +86-21-64250823; E-mail: ruiwang@ecust.edu.cn (RW); Tel: +86-13818862672; E-mail: zhangjian_tina@163.com (JZ); Tel: +86-21-64250213; Fax: +86-21-64250213; E-mail: hlli@ecust.edu.cn (HLL)

References

[1] Rabinovitch M. Molecular pathogenesis of pulmonary arterial hypertension. J Clin Invest 2012; 122: 4306-4313.

[2] Lincoln TM, Dey NB, Boerth NJ, Cornwell TL and Soff GA. Nitric oxide-cyclic GMP pathway regulates vascular smooth muscle cell phenotypic modulation: implications in vascular diseases. Acta Physiol Scand 1998; 164: 507-515.

[3] Christman BW, McPherson CD, Newman JH, King GA, Bernard GR, Groves BM and Loyd JE. An imbalance between the excretion of thromboxane and prostacyclin metabolites in pulmonary hypertension. N Engl J Med 1992; 327: 70-75.

[4] Barnes H, Yeoh HL, Fothergill T, Burns A, Humbert M and Williams T. Prostacyclin for pulmonary arterial hypertension. Cochrane Database Syst Rev 2019; 5: CD012785.

[5] McLaughlin VV, Shah SJ, Souza R and Humbert M. Management of pulmonary arterial hypertension. J Am Coll Cardiol 2015; 65: 1976-1997.

[6] Kenny M, Clarke MM and Pogue KT. Overview of riociguat and its role in the treatment of pulmonary hypertension. J Pharm Pract 2022; 35: 437-444.

[7] Thenappan T, Ormiston ML, Ryan JJ and Archer SL. Pulmonary arterial hypertension: pathogenesis and clinical management. BMJ 2018; 360: j5492.

[8] Humbert M, Guignabert C, Bonnet S, Dorfmüller P, Klinger JR, Nicolls MR, Olschewski AJ, Pullamsetti SS, Schermuly RT, Stenmark KR and Rabinovitch M. Pathology and pathobiology of pulmonary hypertension: state of the art and research perspectives. Eur Respir J 2019; 53: 1801887.

[9] Wang S, Cao W, Gao S, Nie X, Zheng X, Xing Y, Chen Y, Bao H and Zhu D. TUG1 regulates pulmonary arterial smooth muscle cell proliferation in pulmonary arterial hypertension. Can J Cardiol 2019; 35: 1534-1545.

[10] Zhou W, Dasgupta C, Negash S and Raj JU. Modulation of pulmonary vascular smooth muscle cell phenotype in hypoxia: role of cGMP-dependent protein kinase. Am J Physiol Lung Cell Mol Physiol 2007; 292: L1459-L1466.

[11] Guignabert C, Tu L, Le Hiress M, Ricard N, Sattler C, Seferian A, Huertas A, Humbert M and Montani D. Pathogenesis of pulmonary arterial hypertension: lessons from cancer. Eur Respir Rev 2013; 22: 543-551.

[12] Schermuly RT, Stasch JP, Pullamsetti SS, Middendorff R, Müller D, Schlüter KD, Dingendorf A, Hackemack S, Kolosionek E, Kaulen C, Dumitrascu R, Weissmann N, Mittendorf J, Klepetko W, Seeger W, Ghofrani HA and Grimminger F. Expression and function of soluble guanylate cyclase in pulmonary arterial hypertension. Eur Respir J 2008; 32: 881-891.

[13] Lee JH, Tammela T, Hofree M, Choi J, Marjanovic ND, Han S, Canner D, Wu K, Paschini M, Bhang DH, Jacks T, Regev A and Kim CF. Anatomically and functionally distinct lung mesenchymal populations marked by Lgr5 and Lgr6. Cell 2017; 170: 1149-1163, e12.

[14] Shankman LS, Gomez D, Cherepanova OA, Salmon M, Alencar GF, Haskins RM, Swiatlowska P, Newman AA, Greene ES, Straub AC, Isakson B, Randolph GJ and Owens GK. Corrigendum: KLF4-dependent phenotypic modulation of smooth muscle cells has a key role in atherosclerotic plaque pathogenesis. Nat Med 2016; 22: 217.

[15] Grimminger F, Weimann G, Frey R, Voswinckel R, Thamm M, Bölkow D, Weissmann N, Mück W, Unger S, Wensing G, Schermuly RT and Ghofrani HA. First acute haemodynamic study of soluble guanylate cyclase stimulator riociguat in pulmonary hypertension. Eur Respir J 2009; 33: 785-792.

[16] Coghlan JG, Picken C and Clapp LH. Selexipag in the management of pulmonary arterial hypertension: an update. Drug Healthc Patient Saf 2019; 11: 55-64.

[17] Moiseenko A, Vazquez-Armendariz AI, Kheirollahi V, Chu X, Tata A, Rivetti S, Günther S, Lebrigand K, Herold S, Braun T, Mari B, De Langhe S, Kwapiszewska G, Günther A, Chen C, Seeger W, Tata PR, Zhang JS, Bellusci S and El Agha E. Identification of a repair-supportive mesenchymal cell population during airway epithelial regeneration. Cell Rep 2020; 33: 108549.

[18] Habermann AC, Gutierrez AJ, Bui LT, Yahn SL, Winters NI, Calvi CL, Peter L, Chung MI, Taylor CJ, Jetter C, Raju L, Roberson J, Ding G, Wood L, Sucre JMS, Richmond BW, Serezani AP, McDonnell WJ, Mallal SB, Bacchetta MJ, Loyd JE, Shaver CM, Ware LB, Bremner R, Walia R, Blackwell TS, Banovich NE and Kropski JA. Single-cell RNA sequencing reveals profibrotic roles of distinct epithelial and mesenchymal lineages in pulmonary fibrosis. Sci Adv 2020; 6: eaba1972.

[19] McLaughlin VV, Archer SL, Badesch DB, Barst RJ, Farber HW, Lindner JR, Mathier MA, McGoon MD, Park MH, Rosenson RS, Rubin LJ, Tapson VF, Varga J, Harrington RA, Anderson JL, Bates ER, Bridges CR, Eisenberg MJ, Ferrari VA, Grines CL, Hlatky MA, Jacobs AK, Kaul S, Lichtenberg RC, Lindner JR, Moliterno DJ, Mukherjee D, Pohost GM, Rosenson RS, Schofield RS, Shubrooks SJ, Stein JH, Tracy CM, Weitz HH and Wesley DJ. ACCF/AHA 2009 expert consensus document on pulmonary hypertension: a report of the American College of Cardiology Foundation Task Force on Expert Consensus Documents and the American Heart Association: developed in collaboration with the American College of Chest Physicians,

American Thoracic Society, Inc., and the Pulmonary Hypertension Association. Circulation 2009; 119: 2250-2294.
[20] Benza RL, Park MH, Keogh A and Girgis RE. Management of pulmonary arterial hypertension with a focus on combination therapies. J Heart Lung Transplant 2007; 26: 437-446.
[21] Harris DM, Stancampiano FF, Burton MC, Moyer AM, Schuh MJ, Valery JR and Bi Y. Use of Pharmacogenomics to guide proton pump inhibitor therapy in clinical practice. Dig Dis Sci 2021; 66: 4120-4127.
[22] Nelson C, Lee J, Ko K, Sikora AG, Bonnen MD, Enkhbaatar P and Ghebre YT. Therapeutic efficacy of esomeprazole in cotton smoke-induced lung injury model. Front Pharmacol 2017; 8: 16.
[23] Sasaki T, Nakayama K, Yasuda H and Yamaya M. A new strategy with proton pump inhibitors for the prevention of acute exacerbations in COPD. Ther Adv Respir Dis 2011; 5: 91-103.
[24] Canitano A, Iessi E, Spugnini EP, Federici C and Fais S. Proton pump inhibitors induce a caspase-independent antitumor effect against human multiple myeloma. Cancer Lett 2016; 376: 278-283.
[25] Lee JS, Ryu JH, Elicker BM, Lydell CP, Jones KD, Wolters PJ, King TE Jr and Collard HR. Gastroesophageal reflux therapy is associated with longer survival in patients with idiopathic pulmonary fibrosis. Am J Respir Crit Care Med 2011; 184: 1390-1394.
[26] Ghebremariam YT, Cooke JP, Gerhart W, Griego C, Brower JB, Doyle-Eisele M, Moeller BC, Zhou Q, Ho L, de Andrade J, Raghu G, Peterson L, Rivera A and Rosen GD. Pleiotropic effect of the proton pump inhibitor esomeprazole leading to suppression of lung inflammation and fibrosis. J Transl Med 2015; 13: 249-249.
[27] Das M, Dempsey EC, Reeves JT and Stenmark KR. Selective expansion of fibroblast subpopulations from pulmonary artery adventitia in response to hypoxia. Am J Physiol Lung Cell Mol Physiol 2002; 282: L976-986.
[28] Hopper RK, Moonen JR, Diebold I, Cao A, Rhodes CJ, Tojais NF, Hennigs JK, Gu M, Wang L and Rabinovitch M. In pulmonary arterial hypertension, reduced BMPR2 promotes endothelial-to-mesenchymal transition via HMGA1 and its target slug. Circulation 2016; 133: 1783-1794.
[29] Salabei JK and Hill BG. Implications of autophagy for vascular smooth muscle cell function and plasticity. Free Radic Biol Med 2013; 65: 693-703.
[30] Sheikh AQ, Misra A, Rosas IO, Adams RH and Greif DM. Smooth muscle cell progenitors are primed to muscularize in pulmonary hypertension. Sci Transl Med 2015; 7: 308ra159.
[31] Davie NJ, Gerasimovskaya EV, Hofmeister SE, Richman AP, Jones PL, Reeves JT and Stenmark KR. Pulmonary artery adventitial fibroblasts cooperate with vasa vasorum endothelial cells to regulate vasa vasorum neovascularization: a process mediated by hypoxia and endothelin-1. Am J Pathol 2006; 168: 1793-1807.
[32] Kovacic JC, Dimmeler S, Harvey RP, Finkel T, Aikawa E, Krenning G and Baker AH. Endothelial to mesenchymal transition in cardiovascular disease: JACC state-of-the-art review. J Am Coll Cardiol 2019; 73: 190-209.
[33] Good RB, Gilbane AJ, Trinder SL, Denton CP, Coghlan G, Abraham DJ and Holmes AM. Endothelial to mesenchymal transition contributes to endothelial dysfunction in pulmonary arterial hypertension. Am J Pathol 2015; 185: 1850-1858.
[34] Qiao L, Nishimura T, Shi L, Sessions D, Thrasher A, Trudell JR, Berry GJ, Pearl RG and Kao PN. Endothelial fate mapping in mice with pulmonary hypertension. Circulation 2014; 129: 692-703.
[35] Kumar ME, Bogard PE, Espinoza FH, Menke DB, Kingsley DM and Krasnow MA. Mesenchymal cells. Defining a mesenchymal progenitor niche at single-cell resolution. Science 2014; 346: 1258810.
[36] Mayeux JD, Pan IZ, Dechand J, Jacobs JA, Jones TL, McKellar SH, Beck E, Hatton ND and Ryan JJ. Management of pulmonary arterial hypertension. Curr Cardiovasc Risk Rep 2021; 15: 2.
[37] Galiè N, Müller K, Scalise AV and Grünig E. Patent plus: a blinded, randomised and extension study of riociguat plus sildenafil in pulmonary arterial hypertension. Eur Respir J 2015; 45: 1314-1322.
[38] Klinger JR, Chakinala MM, Langleben D, Rosenkranz S and Sitbon O. Riociguat: clinical research and evolving role in therapy. Br J Clin Pharmacol 2020; 87: 2645-2662.
[39] Pasternak B and Hviid A. Use of proton-pump inhibitors in early pregnancy and the risk of birth defects. N Engl J Med 2010; 363: 2114-2123.
[40] Matok I, Levy A, Wiznitzer A, Uziel E, Koren G and Gorodischer R. The safety of fetal exposure to proton-pump inhibitors during pregnancy. Dig Dis Sci 2012; 57: 699-705.

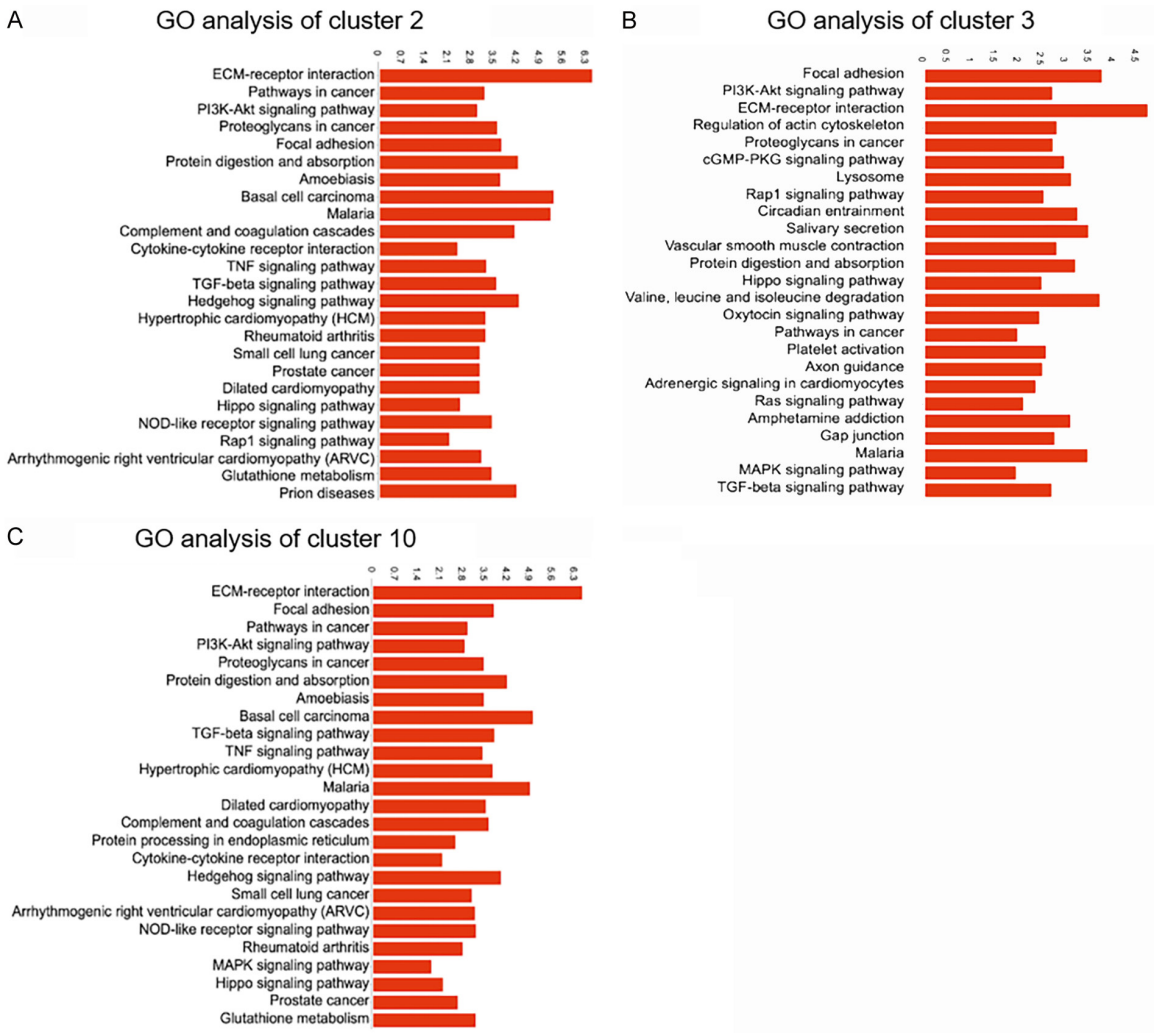

Figure S1. GO analysis of cell cluster 2, 3 and 10. A. GO analysis of cell cluster 2. B. GO analysis of cell cluster 3. C. GO analysis of cell cluster 10.